J. Fluid Mech. (1987), *vol.* 177, *pp.* 19–35
Printed in Great Britain

An asymptotic theory of wind-tunnel-wall interference on subsonic slender bodies

By N. D. MALMUTH
Rockwell International Science Center, Thousand Oaks, CA 91360, USA

(Received 11 November 1985)

An asymptotic theory of solid cylindrical wind-tunnel-wall interference about subsonic slender bodies has been developed. The basic approximation used is one of large wall-radius to body-length ratio. Matched asymptotic expansions show that in contrast to the analogous two-dimensional problem of a confined airfoil, three regions exist. Besides the incompressible crossflow and nearly axisymmetric zones, a wall layer exists where reflection in the wall of the line source representing the body becomes of dominant importance. From the theory, the interference pressures are shown to be approximately constant for closed bodies. Also demonstrated is that D'Alembert's paradox holds for interference drag of such shapes. Numerical studies comparing the exact theory to the asymptotic model which provides drastic simplifications, show that the latter can be used with reasonable accuracy to describe flows, even where the characteristic tunnel-radius to body-length ratio is as low as 1.5.

1. Introduction

Wind-tunnel testing provides a vital tool in the design and development of atmospheric flight vehicles. In spite of the tremendous progress in computational fluid dynamics (CFD), the wind tunnel is needed to simulate phenomena that are otherwise impossible to replicate. Especially difficult issues however arise in modelling of high angle of attack, V/STOL, hypersonic and transonic flows. A major concern in these and other situations is the treatment of wall interference. Because of the highly complex and nonlinear nature of this phenomenon, it represents a challenge to treat even with present CFD methods. This is particularly true in spite of the large body of knowledge built up concerning corrections in linear flow regimes. Accounts of these are given in Garner *et al.* (1966), Pindzola & Lo (1979) and Mokry, Chan & Jones (1983).

The transonic case gives rise to a particularly difficult environment. Some problem areas that contribute to the inaccuracy of wall-interference prediction are:

(i) nonlinearity of the governing equation at supercritical flow conditions;
(ii) nonlinearity of ventilated wall crossflow boundary conditions and difficulties in predicting or measuring them;
(iii) wind-tunnel geometry features, such as finite ventilated wall length, diffuser entry and presence of a wake survey rake and its support;
(iv) boundary layer on tunnel sidewalls, which causes the flow to deviate from two-dimensional test conditions when they are desired.

In addition to these, other viscous effects such as shock–boundary layer interactions are relevant to interference assessment considerations.

To deal with the nonlinear effects, computational procedures have to be utilized

to treat the interaction of the test article with the walls. As a concurrent approach, techniques based on the measurement of flow quantities such as the pressure and velocity components are gaining acceptance. Mokry *et al.* (1974) and Lo (1978) have indicated early applications of this concept. Kraft & Dahm (1982) and Sickles & Kraft (1982) have developed an ingenious 'two variable' technique using this idea for linear subsonic flows. The thrust is to employ experimental observables to account for deviations from the classical homogeneous wall-boundary condition, and as a means of indirectly treating viscous interactions with the wall and model. Within the theoretical framework used, it also bypasses the need for an analytical synthesis of the effective test-article shape.

For the transonic case, there is a need for approaches that can reduce the number of input parameters necessary to compute the correction, shed light on the physics of the wall-interference phenomena, simplify the necessary computations, and be generalized in three dimensions, as well as unsteady flows. Asymptotic procedures such as those described in Lifshits & Fonarev (1978), Chan (1980), Blynskaya & Lifshits (1981), and Cole, Malmuth & Zeigler (1982) provide such advantages. Furthermore, they can provide valuable interactions with the other methods to suggest possible improvements, as well as deriving beneficial features from them. Moreover, nonlinear integral theorems, as well as the asymptotic structure of nonlinear integral equations arising in the matching scheme occurring in the asymptotic analysis, could be of use in the procedure of Kraft & Dahm (1982) and Sickles & Kraft (1982).

Another possibility for accelerating the determination of the corrections and making a quick assessment of whether it is feasible to alter test conditions to make the experiment interference-free is to combine the asymptotic and computational procedures. This approach has merit in treating not only the so-called classical homogeneous wall-boundary conditions, but also those in which experimentally measured pressures are specified on control surfaces. Such a combination can simplify and reduce the computational intensity of the numerical problem through the simplification of the governing equations. In addition, it can help to resolve difficult grid-generation issues present in a purely numerical formulation. For understanding the nature of the boundary conditions, matched asymptotics also can be useful, as indicated in Berndt (1977).

Besides a substantial reduction in computational intensity from the purely numerical model, another simplification arising in a combined asymptotic and computational approach is that the analytical dependence of the interference on parameters such as the wall height can be determined. In fact, these parameters can even be separated out from 'canonical' problems that express the essential structure of the interference phenomenon and interference loadings. This simplifies the determination of interference-free configurations. As an example, for the large-wall-height theories of Chan (1980), and Cole, Malmuth & Zeigler (1982), it is the height–parameter dependence that can be obtained from the underlying asymptotic expansions.

Application of asymptotic procedures to the incompressible and transonic wall interference for porous walls was first considered by Chan (1980) for two-dimensional flows. Therein, no attempt was made to obtain quantitative results with this theory. Studies for a free-stream Mach number near unity are described in Lifshits & Fonarev (1978), and Blynskaya & Lifshits (1981) using similarity solutions applicable in that regime. The case of solid walls in a transonic two-dimensional framework was described in Cole *et al.* (1982). Quantitative results involving a combined

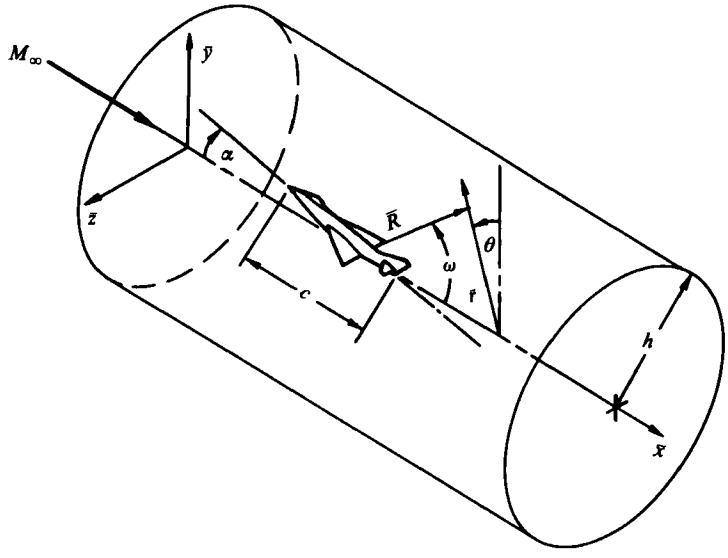

FIGURE 1. Slender vehicle confined inside cylindrical wind-tunnel walls indicating Cartesian, cylindrical and spherical polar coordinates used in analysis.

computational–asymptotic model were presented which gave indications of the accuracy of the theory and its usefulness for the determination of interference-free conditions. This is particularly important in concepts using 'adaptive' or so-called 'smart' wind tunnels in which the walls are configured to achieve near free-field conditions. As described in Lock & Beavan (1944), Ferri & Baronti (1973), Sears (1974), and Parker & Erickson (1982), the adaptive approach involves an iterative adjustment of the wall shape with a feedback loop involving a prediction of the wall–model interaction, which may be based on a computational simulation. It is therefore evident that the practical feasibility of the method depends on the rapidity of response of the predictive part of the smart-wall procedure.

To handle practical conditions such as these with the asymptotic method, three-dimensional simulations are required. The analytical framework extending the analysis of Cole *et al.* (1982) to the three-dimensional transonic cases is given in Malmuth & Cole (1984). For the purposes of determining how the three-dimensional theory can be applied and of obtaining quantitative information, the case of subsonic flow will be described in this paper. This is important, since the theory has some similarities with that for the transonic case described in Malmuth & Cole (1984). Moreover, the underlying linear framework simplifies the study of the quantitative relationship between the finite-height interference problem and the large-height asymptotic approximation. In this manner, the range of applicability in terms of the height parameter can be carefully studied with possible implications for the transonic case. This is particularly important when moderate height to model-size ratios are considered to minimize viscous scale effect.

2. Overview of approach

The basic configuration to be treated is shown in figure 1, which shows a slender vehicle confined by cylindrical solid walls. A front view of this arrangement is shown in figure 2. Also, schematically indicated there is the basic asymptotic structure of

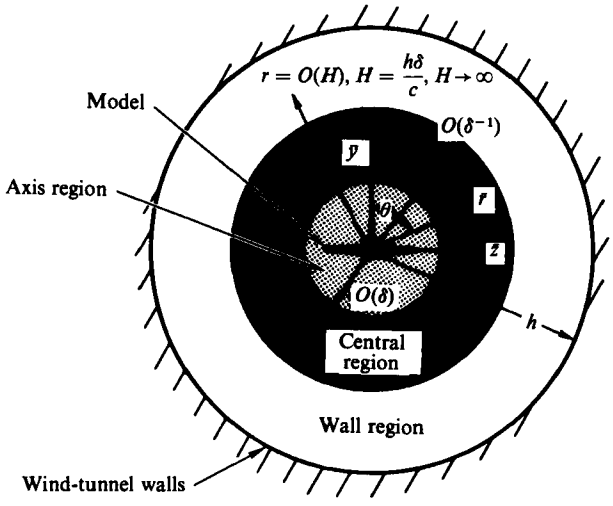

FIGURE 2. Front view of wind-tunnel model confined by cylindrical walls, showing regions of applicability of asymptotic expansions.

the problem. If h represents the wall height, and c a characteristic model dimension, $H = h/c$ is a parameter which is to be considered large in the theory. In this approximation, three regions of dramatically different structure emerge. If the characteristic model thickness ratio δ is small compared to unity, classical slender-body theory described in Cole (1968) holds to dominant order in a zone away from the walls. This region can be subdivided into subdomains denoted in figure 2 as the central and axis regions. In the former, the effect of asymmetry associated with an arbitrary slender aircraft at incidence becomes unimportant and it can be modelled as a line source. For the latter, crossflow gradients dominate, and the flow is harmonic in planes perpendicular to the free-stream direction. The effect of the walls in the central and axis regions is felt as a weak perturbation about the dominant slender-body flow field. The essential task is to predict interference pressure and loading associated with this wall perturbation. In this connection, a singular perturbation problem results, since the approximation of weak wall-induced perturbations becomes invalid near the walls. In this zone, denoted as the wall region in figure 2, the flow is dominantly that of a line source reflected in the walls.

In this paper, the application of an asymptotic matching procedure will be demonstrated to derive representations for the velocity potential Φ in all three of the layers. This technique exploits the property that each of these representations has an overlap domain of validity. From this feature, it is possible to compare unknown elements near the interface of each of the zones and determine them.

3. Formulation

3.1. *Exact problem* ($h < \infty$)

Before discussing the asymptotic theory, the 'exact' problem will be treated. In this paper, the term exact refers to finite height ($h < \infty$) walls interacting with a slender model. A more general situation refers to non-slender models, which will be deferred to a future discussion.

3.2. *Slender-body approximations*

The flow over a slender aircraft wind-tunnel model shown in figure 1 is considered in which the surface of the test article is given by

$$B = r - \delta F(x, \theta) = 0, \tag{1}$$

in cylindrical coordinates. In the notation of figure 1, normalized coordinates,

$$x = \frac{\bar{x}}{c}, \quad r = \frac{\bar{r}}{c} \tag{2}$$

(in which c is a characteristic body length) are introduced, and the bars signify dimensional quantities.

A representation of the velocity potential Φ within incompressible small-disturbance theory is given by the following asymptotic expansion:

$$\frac{\Phi}{U} = \bar{x} + \nu(\delta)\,\phi(x, r; H, A) + \ldots, \tag{3}$$

that is an approximate representation of Φ in an 'outer' limit,

$$x, r, H = \frac{h}{c}, \quad A = \frac{\alpha}{\delta} \text{ fixed} \quad \text{as } \delta \to 0, \tag{4}$$

which applies in some region away from the x-axis (axis or inner region), i.e. in the central region, previously identified and shown in figure 2. Here, U is the free-stream velocity, α = angle of attack, δ = characteristic thickness ratio, $\boldsymbol{q}$ = velocity = $\nabla\Phi$. Although this formulation will be incompressible, all the arguments can be easily generalized to a subsonic Prandtl–Glauert framework.

For solid cylindrical wind-tunnel walls, the expansion (3) anticipates that the flow becomes quickly axisymmetric away from an asymmetric body. As will be seen from matching, the zone of asymmetry is $O(\delta)$.

The exact equation of the velocity potential is

$$\Delta\Phi = \Phi_{xx} + \frac{1}{r}(r\Phi_r)_r + \frac{1}{r^2}\Phi_{\theta\theta} = 0. \tag{5a}$$

The solid tunnel-wall boundary condition is

$$\frac{\partial\Phi}{\partial r}(x, H) = 0. \tag{5b}$$

Substitution of (3) into (5a) and retaining like orders gives the problem

$$\left[\frac{\partial^2}{\partial x^2} + \frac{1}{r}\frac{\partial}{\partial r}\left(r\frac{\partial}{\partial r}\right)\right]\phi = 0, \tag{6a}$$

$$\frac{\partial\phi(x, H)}{\partial r} = 0. \tag{6b}$$

A complete specification of this problem requires a matching condition with the axis region. To keep the body in view in the limit $\delta \to 0$, a strained coordinate $r^* = r/\delta$ must be held fixed in this limit. In the axis zone, the potential is assumed to have the expansion

$$\frac{\Phi}{U} = x + \mu_{\frac{1}{2}}(\delta)\,\phi^*_{\frac{1}{2}}(x) + \mu_1(\delta)\,\phi^*(x, r^*, \theta) + \ldots, \tag{7}$$

which holds for the 'inner' limit

$$x, r^*, H, A \text{ fixed} \quad \text{as } \delta \to 0, \tag{8}$$

where, without loss of generality, the body length has been set to unity. In (7) the second term is a 'switchback' term which has been inserted to facilitate matching. On substitution of (7) into (5a), the equation governing ϕ^* can be obtained as:

$$\frac{1}{r^*}\frac{\partial}{\partial r^*}\left(r^*\frac{\partial \phi^*}{\partial r^*}\right)+\frac{1}{r^{*2}}\frac{\partial^2 \phi^*}{\partial \theta^2}=0. \tag{9}$$

As indicated in Malmuth & Cole (1984), Cole (1968) and Cole (1972), the formulation for (9) is completed by the condition of flow tangency and matching. The former is written as

$$\boldsymbol{q}\cdot\boldsymbol{\nabla} B = 0, \tag{10}$$

where $\boldsymbol{q}$ = velocity = $\boldsymbol{\nabla}\Phi$. The most general boundary condition for which $\partial\phi^*/\partial\theta = O(\partial\phi^*/\partial r)$ is obtained if

$$\mu_1 = \delta^2.$$

Further, (10) implies that

$$\frac{\partial \phi^*}{\partial n} = \frac{FF_x}{(F^2+F_\theta^2)^{\frac{1}{2}}}, \tag{11}$$

where n is the normal to the boundary for the harmonic crossflow problem associated with (9) and (11) shown in figure 3. In the notation of figure 1, this is an x = constant cross-section of the test article. Assuming no yaw and lateral asymmetry, i.e. $\phi^*(r^*, \theta, x) = \phi^*(r^*, -\theta; x)$, the most appropriate solution of (9) and (11) is

$$\phi^* = \mathscr{P}^*(x)\ln r^* + g^*(x) + \sum_{n=1}^{\infty}\frac{g_n^*(x)\cos n\theta}{r^{*n}}. \tag{12}$$

Equation (12) provides the essential relation in matching the inner and outer expansions. For matching, an intermediate variable is introduced so that inner and outer solutions can be written in an overlap domain of common validity. The purpose of this step is to determine unknown elements in each, such as $\mathscr{P}^*(x)$ in (12) and $\mu_{\frac{1}{2}}$ in (7). If the order of magnitude relation

$$\delta \ll \eta(\delta) \ll 1,$$

holds, where $\delta \ll \eta(\delta)$ signifies $O(\eta(\delta)) > O(\delta)$, then an intermediate limit in which

$$r_\eta = \frac{r}{\eta(\delta)} \quad \text{is fixed as } \delta \to 0, \tag{13}$$

is defined. The outer expansion written in these intermediate variables is

$$\frac{\Phi_{\text{outer}}}{U} = x + \nu(\phi)\{\mathscr{P}(x)\ln(\eta r_\eta) + g(x)\} + \ldots, \tag{14}$$

and the inner is

$$\frac{\Phi_{\text{inner}}}{U} = x + \mu_{\frac{1}{2}}(\delta)\phi_{\frac{1}{2}}(x) + \delta^2\{\mathscr{P}^*(x)[\ln(\eta r_\eta) - \ln\delta + g_0^*(x)]\}, \tag{15}$$

where in (14) it is assumed for purposes of matching that

$$\phi(x, r) \approx \mathscr{P}(x)\ln r + g(x), \tag{16}$$

as $r \to 0$.

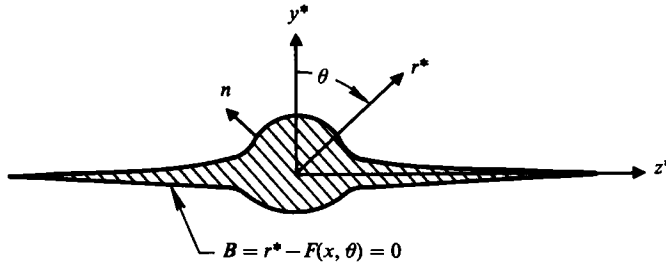

FIGURE 3. Crossflow plane geometry.

By Gauss' theorem, $\mathscr{P}^*(x) = S'(x)/2\pi$, where

$$S(x) = \frac{1}{2}\oint F^2\,\mathrm{d}s,$$

and s is the arc length along boundary B in figure 3. The quantity $S(x)$ is the local cross-sectional area. For a closed contour

$$S(x) = \frac{1}{2}\int_0^{2\pi} F^2\,\mathrm{d}\theta. \tag{17}$$

On comparison of (14) and (15), matching gives

$$\left.\begin{aligned} \mu_{\frac{1}{2}} &= \delta^2 \ln\delta \quad \nu(\delta) = \delta^2, \\ \phi_{\frac{1}{2}} &= \mathscr{P}^*(x) = \frac{S'(x)}{2\pi} g_0^* = g(x). \end{aligned}\right\} \tag{18}$$

Equations (16) and (18) provide the necessary completion of the specification of the outer problem. It should be noted that these results are identical so far to those obtained for symmetrical unconfined bodies of revolution obtained in Cole (1968). The effects of asymmetry represented by the multipole last term in (12) are higher order in (15). As will be seen, the significance of this result is that the interference effect of the walls on a confined asymmetric body is axisymmetric.

On the basis of the matching condition, (16) can be written in the flux form

$$\lim_{r\to 0}(r\phi_r) = \frac{S'(x)}{2\pi}. \tag{16'}$$

The solution of (6) for ϕ can be obtained as a line source reflected in the solid cylindrical wind-tunnel walls. The exponential Fourier transform method applied in Malmuth & Cole (1984) can be used to obtain a Green function, satisfying appropriate conditions for this representation. The line source is a convolution of this Green function. Accordingly, if $0 \leqslant x \leqslant 1$,

$$\phi = I_1 + I_2, \tag{19a}$$

$$2\pi H^2 I_1 = \int_0^1 |x-\xi| S'(\xi)\,\mathrm{d}\xi, \tag{19b}$$

$$I_2 = I_{21} + I_{22}, \tag{19c}$$

$$4\pi^2 I_{21} = \int_0^1 S'(\xi)\,\mathrm{d}\xi \int_{-\infty}^{\infty} \mathrm{e}^{\mathrm{i}k(x-\xi)}\left\{\frac{2}{k^2H^2} - \frac{K_1(kH)\,I_0(kr)}{I_1(kH)}\right\}\mathrm{d}k, \tag{19d}$$

$$4\pi^2 I_{22} = -\int_0^1 S'(\xi)\,\mathrm{d}\xi \int_{-\infty}^{\infty} \mathrm{e}^{\mathrm{i}k(x-\xi)} K_0(kr)\,\mathrm{d}k$$

$$= -\int_0^1 \frac{\pi S'(\xi)\,\mathrm{d}\xi}{((x-\xi)^2+r^2)^{\frac{1}{2}}}. \tag{19e}$$

In (19), I_1, K_0 and K_1 signify modified Bessel functions. Writing the solution of the inner problem embodied by (9) and (11) as

$$\phi^* = \hat{\phi} + g(x),$$

then,

$$g = I_1(x) + g_{21}(x) + g_{22}(x),$$

where the method of Cole (1968) can be used to show that

$$\pi^2 g_{21}(x) = \int_0^1 S'(\xi)\,\mathrm{d}\xi \int_0^{\infty} \cos k(x-\xi)\left\{\frac{1}{k^2H^2} - \frac{K_1(kH)}{2I_1(kH)}\right\}\mathrm{d}k,$$

$$-g_{22}(x) = \frac{1}{2\pi} S(x) \ln 2 + \frac{1}{4\pi}\int_0^1 S'(\xi)\,\mathrm{sgn}\,(x-\xi)\ln|x-\xi|\,\mathrm{d}\xi.$$

Using Bernoulli's theorem, the pressure coefficient C_{P_B} on the body is given by

$$-\frac{C_{P_B}}{2\delta^2} = (\ln\delta)\frac{S''(x)}{2\pi} + \hat{\phi}_x + g'(x) + \tfrac{1}{2}|\nabla_T \hat{\phi}|^2, \tag{20}$$

where

$$|\nabla_T \hat{\phi}|^2 = \left(\frac{\partial\hat{\phi}}{\partial r^*}\right)^2 + \frac{1}{F^2}\left(\frac{\partial\hat{\phi}}{\partial\theta}\right)^2.$$

For an axisymmetric body, i.e. $F_\theta = 0$, and

$$-\frac{C_{P_B}}{2\delta^2} = \frac{S''(x)}{2\pi}\ln\delta F + g'(x) + \tfrac{1}{2}F'^2.$$

In accord with the previous discussion, the free-field pressure coefficient $C^{\infty}_{P_B}$ corresponds to $g = g_{22}$ in (20). Therefore, the interference pressure $\Delta C_{P_B} \equiv C_{P_B} - C^{\infty}_{P_B}$ is

$$-\frac{\Delta C_{P_B}}{2\delta^2} = g_{21_x}(x;H) + I_1'(x) = \frac{1}{2\pi^2 H^3}\int_0^1 S'(\xi)\,\mathrm{d}\xi \int_0^{\infty} t\sin\frac{t(x-\xi)}{H}\frac{K_1(t)}{I_1(t)}\mathrm{d}t. \tag{21}$$

In summary, (21) is an area rule for wind-tunnel-wall interference from slender-body theory. It indicates that the interference pressure on the body depends only on x, H and $S(x)$, and is independent of the body cross-sectional shape variation.

3.3. *Large height* ($h \to \infty$) *theory*

3.3.1. *Central layer*

In this region, the asymptotic representation for ϕ is assumed to be

$$\phi_{\text{central}} = \mu_0(H)\,\phi_0(x,r) + \mu_1(H)\,\phi_1(x,r) + \ldots, \tag{22}$$

for the central layer limit

$$r \text{ fixed as } \quad H \to \infty. \tag{23}$$

Substitution of (22) into (6a) gives

$$\left[\frac{\partial^2}{\partial x^2} + \frac{1}{r}\frac{\partial}{\partial r}\left(r\frac{\partial}{\partial r}\right)\right]\phi_{0,1} = 0, \tag{24}$$

and a similar process applied to the boundary condition (16′) gives

$$\lim_{r\to 0} r\frac{\partial \phi_0}{\partial r} = \frac{S'(x)}{2\pi}, \tag{25a}$$

$$\lim_{r\to 0} r\frac{\partial \phi_1}{\partial r} = 0. \tag{25b}$$

Under the assertion (to be validated by matching) that $\mu_0 = 1$, and ϕ_0 represents the free field,

$$\phi_0 = I_{22} = -\frac{1}{4\pi}\sum_{n=0}^{\infty}\frac{P_n(\cos\omega)}{R^{n+1}}\bar{I}_n, \tag{26}$$

$$\left.\begin{aligned} \bar{I}_n &\equiv \int_0^1 \xi^n S'(\xi)\,\mathrm{d}\xi, \\ R &= \bar{R}/c = (x^2+r^2)^{\frac{1}{2}}, \end{aligned}\right\} \tag{27}$$

where the P_n are Legendre polynomials, ω is the polar angle defined in figure 1, and the $\bar{I}_n$ represents area derivative moments. Equation (26) is inconsistent with the wall boundary condition (5*b*). Accordingly, another asymptotic expansion is required in the vicinity of the walls.

3.3.2. *Wall layer*

The perturbation potential near the wall is assumed to have the following form:

$$\phi_{\text{wall}} = \epsilon_0(H)\,\varphi_0(x^\dagger, r^\dagger) + \epsilon_1(H)\,\varphi_1(x^\dagger, r^\dagger) + \ldots, \tag{28}$$

which is valid in the wall-layer limit

$$x^\dagger = \frac{x}{H}, \quad r^\dagger = \frac{r}{H}, \quad \text{fixed as } H\to\infty. \tag{29}$$

By the substitution procedure previously described, the wall-layer approximation can be shown to satisfy the following hierarchy:

$$\left[\frac{\partial^2}{\partial x^{\dagger 2}} + \frac{1}{r^\dagger}\frac{\partial}{\partial r^\dagger}\left(r^\dagger\frac{\partial}{\partial r^\dagger}\right)\right]\varphi_0 = S(1)\,\delta(x^\dagger)\frac{\delta^+(r^\dagger)}{2r^{\dagger 2}}, \tag{30a}$$

$$\left[\frac{\partial^2}{\partial x^{\dagger 2}} + \frac{1}{r^\dagger}\frac{\partial}{\partial r^\dagger}\left(r^\dagger\frac{\partial}{\partial r^\dagger}\right)\right]\varphi_1 = 0, \tag{30b}$$

where $\delta(x^\dagger)$ and $\delta^+(r^\dagger)$ are the full and half delta functions. The forcing term in (30*a*) is associated with the singular behaviour $\varphi_0 \approx -S(1)/4\pi R^\dagger + \ldots$ as $R^\dagger \to 0$, where $R^\dagger = R/H$. This is based on matching requirements with ϕ_0. The φ_0 solution is similar to that associated with the transonic theory discussed in Malmuth & Cole (1984). It is a reflection of point source of strength proportional to the base area $S(1)$ in the solid cylindrical tunnel walls, and is given as

$$\varphi_0 = S(1)\left\{\frac{x^\dagger}{2\pi}\operatorname{sgn} x^\dagger + M\right\}, \tag{31a}$$

$$M = M_0 + M_1, \tag{31b}$$

$$M_0 = -\frac{1}{2\pi^2}\int_0^\infty \cos kx^\dagger K_0(kr^\dagger)\,\mathrm{d}k, \tag{31c}$$

$$M_1 = \frac{1}{\pi}\int_0^\infty \cos kx^\dagger\left\{\frac{1}{\pi k^2} - \frac{K_1(k)\,I_0(kr^\dagger)}{2\pi I_1(k)}\right\}\mathrm{d}k. \tag{31d}$$

Using methods given in Malmuth & Cole (1984), these integrals can be approximated for $R^\dagger \to 0, \omega$ fixed to give the following singular representation of φ_0 in that limit:

$$\varphi_0 = S(1)\left\{-\frac{1}{4\pi R^\dagger} + a_0 + b_0 R^{\dagger 2} P_2(\cos\omega) + \ldots\right\}, \tag{32}$$

where

$$a_0 = \frac{1}{\pi^2}\int_0^\infty \left\{\frac{1}{k^2} - \frac{K_1(k)}{2I_1(k)}\right\} \mathrm{d}k = 0.12955, \tag{33a}$$

$$b_0 = \frac{1}{4\pi^2}\int_0^\infty \frac{k^2 K_1(k)}{I_1(k)} \mathrm{d}k = 0.063409. \tag{33b}$$

The integrals in (33a) and (33b) are convergent, can be evaluated once and for all numerically, and are independent of $x^\dagger$ and $r^\dagger$.

The dominant term of (32) is a source and the next two terms represent effects associated with reflections of this singularity in the walls. Based on preliminary matching considerations, stronger singularities such as a dipole and quadrupole are required for the dominant terms of the next higher-order approximations. These are obtained from differentiating (32) with respect to x. They have reflections in the walls given by the higher-order terms of these derivatives. In accord with these ideas, the singular behaviour of ϕ_{wall} as $R^\dagger \to 0$ is

$$\phi_{\text{wall}} = \epsilon_0(H) S(1)\left[\frac{-1}{4\pi R^\dagger} + a_0 + b_0 R^{\dagger 2} P_2(\cos\omega) + \ldots\right]$$
$$+ \epsilon_{\frac{1}{2}}(H) B\left[\frac{\cos\omega}{4\pi R^{\dagger 2}} + 2b_0 R^\dagger \cos\omega \ldots\right] + \epsilon_1(H) C\left[\frac{-1}{2\pi}\frac{P_2(\cos\omega)}{R^{\dagger 3}} + 2b_0 + \ldots\right]. \tag{34}$$

Also based on preliminary matching considerations, switchback terms are interposed between the dominant and second-order terms in (22) so that

$$\phi_{\text{central}} = \phi_0 + \mu_{\frac{1}{2}}\phi_{\frac{1}{2}} + \mu_{\frac{3}{4}}\phi_{\frac{3}{4}} + \mu_1\phi_1 + \ldots . \tag{35}$$

The added switchback terms (denoted herein by fractional subscripts) are to be determined by matching. In anticipation of this step, a suitable representation for the dominant wall-induced perturbation of the central region perturbation potential ϕ_1 that satisfies (24) and (25b) exactly is

$$\phi_1 = A_{10} R^2 P_2(\cos\omega) + A_{11} R\cos\omega + A_{12}. \tag{36}$$

It is significant to note that the analytical determination of ϕ_1 in (36) illustrates a key distinction between the incompressible case of this paper and the transonic one treated in Malmuth & Cole (1984). Therein, ϕ_1 satisfies a 'variational' equation which is linear perturbation about the nonlinear dominant (free-field) ϕ_0 approximation, and can probably only be solved numerically. The variational equation is essentially the same as that arising in the transonic lifting-line theory developed by Cook & Cole (1978). It can have discontinuous coefficients associated with shocks in the dominant ϕ_0 approximation.

3.3.3. *Matching of central and wall layers*

Following the procedure indicated earlier, unknown elements in the ϕ_{wall} and ϕ_{central} representations are determined by writing each in terms of a suitable

intermediate variable and finding common terms. For this purpose, the appropriate intermediate variable is

$$R_\eta = R/\eta(H), \tag{37}$$

where $1 \ll \eta \ll H$.

The representations of ϕ_{wall} and ϕ_{central} are thus

$$\phi_{\text{central}} = \underset{①}{-\frac{1}{4\pi}\frac{\bar{I}_0}{\eta R_\eta}} + \underset{②}{\frac{\bar{I}_1\cos\omega}{\eta^2 R_\eta^2}} + \underset{③}{\frac{\bar{I}_2 P_2(\cos\omega)}{\eta^3 R_\eta^3}} + \dots$$
$$+ \underset{④}{\mu_{\frac{1}{2}}\phi_{\frac{1}{2}}} + \underset{⑤}{\mu_{\frac{3}{4}}\phi_{\frac{3}{4}}} + \underset{⑥}{\mu_1\{A_{10}\eta^2 R_\eta^2 P_2(\cos\omega)} + \underset{⑦}{A_{11}\eta R_\eta\cos\omega} + \underset{⑧}{A_{12}\}} + \dots \tag{38}$$

$$\phi_{\text{wall}} = \epsilon_0 S(1)\Big[\underset{①'}{-\frac{1}{4\pi(\eta R_\eta/H)}} + \underset{②'}{a_0} + \underset{③'}{b_0\frac{\eta^2 R_\eta^2}{H^2}P_2(\cos\omega)} + \dots\Big]$$
$$+ \epsilon_{\frac{1}{2}} B\Big[\underset{④'}{\frac{\cos\omega}{4\pi(\eta^2 R_\eta^2/H^2)}} + \underset{⑤'}{\phi_0 = 0} + \underset{⑥'}{2b_0\frac{\eta R_\eta}{H}\cos\omega} + \dots\Big]$$
$$+ \epsilon_1(H) C\Big[\underset{⑦'}{-\frac{1}{2\pi}\frac{P_2(\cos\omega)}{\eta^3 R_\eta^3/H^3}} + \underset{⑧'}{2b_0}\Big], \tag{39}$$

where ⑤′ is a dummy term added to elucidate the matching arguments.

On comparison of the various terms in (38) and (39) with the circled labels above them, it can be seen that the following matchings apply:

①′↔①	②′↔④	③′↔⑥	④′↔②	⑤′↔⑤
$\epsilon_0 = 1/H.$	$\mu_{\frac{1}{2}} = 1/H,$	$A_{10} = S(1)\,b_0,$	$B = -\bar{I}_1,$	
	$\phi_{\frac{1}{2}} = S(1)\,a_0.$	$\mu_1 = 1/H^3.$	$\epsilon_{\frac{1}{2}} = 1/H^2.$	

Since there is no constant term in the dipole reflection response to the dipole involving 2 (i.e. $c_0 = 0$),

$$\mu_{\frac{3}{4}} = \phi_{\frac{3}{4}} = 0.$$

⑥′↔⑦	⑦′↔③	⑧′↔⑧
$A_{11} = 2Bb_0,$	$C = \frac{1}{2}\bar{I}_2,$	$A_{12} = 2b_0\,C = b_0\bar{I}_2.$
$A_{11} = -2\bar{I}_1 b_0.$	$\epsilon_1 = 1/H^3.$	

3.3.4. *Matching of central and axis layers*

Based again on preliminary matching requirements which use the information about ϕ_{central} just obtained, the secondary ($H\to\infty$) expansion for ϕ^* in (7) is

$$\phi^*(x, r^*; H) = \phi_0^*(x, r^*) + \tau_{\frac{1}{2}}(H)\,\phi_{\frac{1}{2}}^* + \tau_1(H)\,\phi_1^* + \dots. \tag{40}$$

From the previous section,

$$\phi(x, r; H) = \phi_0 + \frac{a_0 S(1)}{H} + \frac{1}{H^3}\phi_1(x, r) + \dots. \tag{41}$$

Introducing the intermediate variable r_ζ, where

$$\delta \ll \zeta(\delta) \ll 1,$$

then the velocity potential in the central and axis layer is, assuming that

$$\phi_0^* \approx \frac{S'(x)}{2\pi} \ln r^* \quad \text{as } r^* \to \infty,$$

$$\frac{\Phi_{\text{central}}}{U} = x + \delta^2 \left\{ \underset{①'}{\frac{S'(x)}{2\pi} \ln \zeta r_\zeta} + \underset{②'}{g_0(x)} + \underset{③'}{\frac{a_0 S(1)}{H}} + \underset{④'}{\frac{g_1(x)}{H^3}} + \ldots \right\}, \tag{42}$$

$$\frac{\Phi_{\text{axis}}}{U} = x + \cancel{\frac{\delta^2 \ln \delta}{2\pi} S'(x)} + \delta^2 \left\{ \underset{①}{\frac{S'(x)}{2\pi} [\ln \zeta r_\zeta - \cancel{\ln \delta}]} + \underset{②}{g_0^*(x)} + \underset{③}{\tau_{\frac{1}{2}}(H) \phi_{\frac{1}{2}}^*} + \underset{④}{\tau_1(H) \phi_1^* \left(x, \frac{\zeta r_\zeta}{\delta} \right)} + \ldots \right\}. \tag{43}$$

Comparing (41) and (42), the matchings are:

①'↔①	②'↔②	③'↔③	④'↔④
Already matched.	$g_0^* = g_0$.	$\tau_{\frac{1}{2}} = 1/H$, $\phi_{\frac{1}{2}}^* = a_0 S(1)$.	$\tau_1 = 1/H^3$,

$$\phi_1^* \approx g_1(x) = \lim_{r \to 0} \phi_1(x, r).$$

Now, by (36),

$$\lim_{r \to 0} \phi_1 = g_1(x) = b_0 \{ S(1) x^2 - 2\bar{I}_1 x + \bar{I}_2 \}. \tag{44}$$

Letting $$\Delta_T = \frac{1}{r^*} \frac{\partial}{\partial r^*} \left(r^* \frac{\partial \phi^*}{\partial r^*} \right) + \frac{1}{r^{*2}} \frac{\partial^2 \phi^*}{\partial \theta^2},$$

substitution of (40) into (9) and (11) gives

$$\Delta_T \phi_{0,1}^* = 0, \tag{45}$$

$$\frac{\partial \phi_0^*}{\partial n} = \frac{F F_x}{(F^2 + F_\theta^2)^{\frac{1}{2}}}, \tag{46}$$

$$\frac{\partial \phi_1^*}{\partial n} = 0. \tag{47}$$

On the basis of previous work,

$$\phi_0^* = \frac{S'(x)}{2\pi} \ln r^* + g_0(x) \quad \text{as } r^* \to \infty, \tag{48}$$

and $$g_0(x) = g_{22}(x).$$

In addition,

$$\phi_1^* = g_1, \tag{49}$$

solves (45) and (47) and satisfies the asymptotic matching conditions as $r^* \to \infty$.

Summarizing the previous results, the expansions of the velocity potential in the various regions are:

3.3.5. *Axis region*

$$\frac{\Phi}{U} = x + \frac{\delta^2 \ln \delta}{2\pi} S'(x) + \delta^2 \left\{ \phi_0^*(x, r^*, \theta) + \frac{a_0 S(1)}{H} + \frac{\phi_1^*}{H^3} + \ldots \right\} + \ldots, \tag{50a}$$

$r^* = r/\delta$ fixed as $\delta \to 0, H \to \infty$.

3.3.6. *Central region*

$$\frac{\Phi}{U} = x + \delta^2 \left\{ \phi_0(x, r) + \frac{1}{H} a_0 + \frac{1}{H^3} \phi_1(x, r) + \ldots \right\}, \tag{50b}$$

r fixed as $\delta \to 0, H \to \infty$.

3.3.7. *Wall region*

$$\frac{\Phi}{U} = x + \delta^2 \left\{ \frac{1}{H} \varphi_0(x^\dagger, r^\dagger) + \frac{1}{H^2} \varphi_1 + \ldots \right\}, \tag{50c}$$

$$x^\dagger = x/H, r^\dagger = r/H \quad \text{fixed as } \delta \to 0, H \to \infty,$$

where ϕ_1^* is given by (44) and (49), ϕ_0^* solves (45), (46) and (48), ϕ_0 is given by (26), and ϕ_1 by (44). Using the method of Malmuth & Cole (1984) involving the derivation of (32), as a check, it can be shown that ϕ_1 in (50*b*) can be obtained from the exact result for ϕ in (19).

3.4. *Free-field and approximate interference pressures*

From (20) and the subsequent discussion,

$$-\frac{C_{P_B}^{\infty}}{2\delta^2} = \left(\ln \delta\right) \frac{S''(x)}{2\pi} + \hat{\phi}_x + g_{22}(x) + \tfrac{1}{2} |\nabla_T \hat{\phi}|^2, \tag{51}$$

and

$$-\frac{\Delta C_{P_B}}{\delta^2} = \frac{4b_0}{H^3} \{S(1)\, x - \bar{I}_1\}. \tag{52}$$

Thus the approximate theory states that interference pressure is constant for closed bodies to dominant order, is independent of the body cross-sectional shape distribution, and varies linearly with x for open bodies. Equation (52) indicates that the interference pressure falls off rapidly with increasing H due to the strong three-dimensional relief about the confined slender body.

3.5. *Drag*

For an axisymmetric body with a blunt base having a base pressure assumed to be the ambient value P_∞, the drag coefficient C_D based on the base area is

$$C_D = \frac{2}{F^2(1)} \int_0^1 C_p F F' \, \mathrm{d}x. \tag{53}$$

Based on (52) and (53), the approximate interference drag coefficient ΔC_D for a body of revolution is

$$\begin{aligned} \Delta C_D &= -\frac{4b_0 \delta^2}{H^3} \left\{ S(1) \int_0^1 x F F'(x) \, \mathrm{d}x - \int_0^1 F F' \, \mathrm{d}x \int_0^1 \xi S'(\xi) \, \mathrm{d}\xi \right\} + o(1) \\ &= o(1). \end{aligned} \tag{54}$$

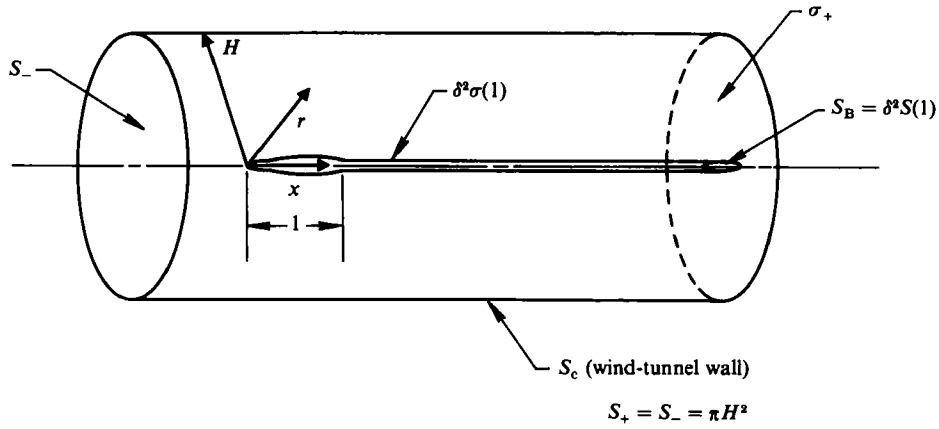

FIGURE 4. Control cylinder for interference drag determination.

Thus, to the order of approximation considered, and with the assumed base pressure, the interference drag coefficient of a confined open axisymmetric body has no dynamic component, but has merely the static value. A similar result holds exactly for open bodies of arbitrary shape with a cylindrical afterbody at infinity in a free field as described in Batchelor (1967).

To determine whether (54) holds for bodies of more general shape and study the o symbol in (54), a momentum theorem analysis is made on the control cylinder of figure 4. If S_+ and S_- are the areas of the end faces of the cylinders, S_c its curved impervious face corresponding to solid walls, and the flow over a slender body in the interval $0 \leqslant x \leqslant 1$ of cross-sectional area $S_B = S(1)$ with a cylindrical afterbody for $x > 1$ is considered, then the momentum theorem for the drag D is

$$D = P(-\infty)S_- - P(\infty)S_+ + \rho_\infty[u^2(-\infty)S_- - u^2(\infty)S_+], \tag{55}$$

where P is the pressure, u is the x-component of the flow velocity on the end faces, and the arguments $\pm\infty$ corresponds to these surfaces. Now, an open body of the type considered behaves as a confined source of strength $S(1)$. Accordingly,

$$\frac{u}{U} \approx 1 \mp \frac{\delta^2 S(1)}{2\pi H^2} + \ldots \quad \text{as } x \to \pm\infty.$$

In accord with Bernoulli's equation and these relations, the drag force D is approximately

$$D = P_\infty \delta^2 S(1) + \frac{\rho_\infty U^2 \delta^4 S^2(1)}{2\pi H^2} + \ldots, \tag{56}$$

where P_∞ and ρ_∞ are the ambient pressure and density. This shows the blockage correction to (54). Denoting P_- and U_- as the pressure and velocity at the upstream face S_- of the control surface of figure 4, the exact result for the drag is from Cole (private communication, 1984)

$$\begin{aligned} D &= P_- S_B - \frac{\rho U_-^2}{2} S_B \left(\frac{\lambda}{1-\lambda}\right), \\ \lambda &= \frac{S_B}{\pi H^2}, \end{aligned} \tag{57}$$

which is consistent with the $O(\delta^4)$ magnitude of the interference drag determined by the approximate theory given in (56), and checks (56) allowing for the confined source

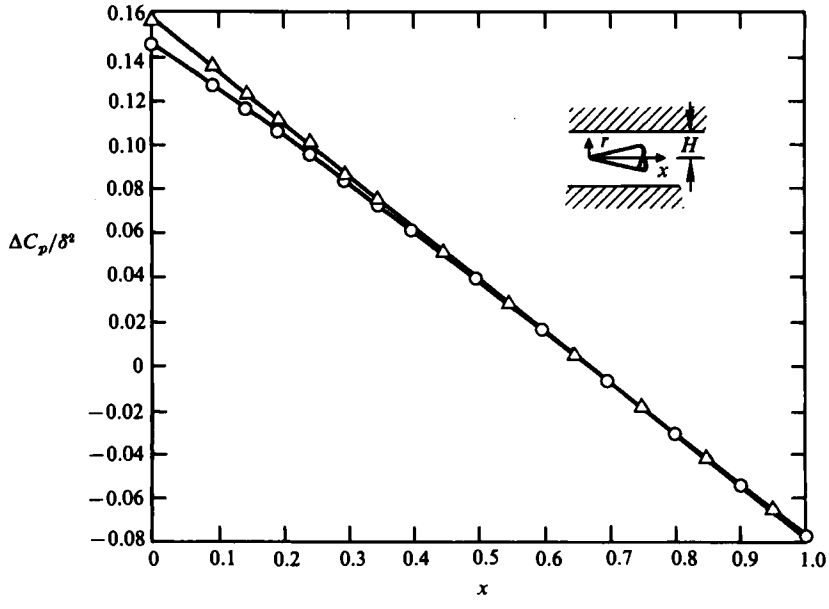

FIGURE 5. ○, exact and △, approximate interference pressures for cone ($F = x$), $H = 1.5$.

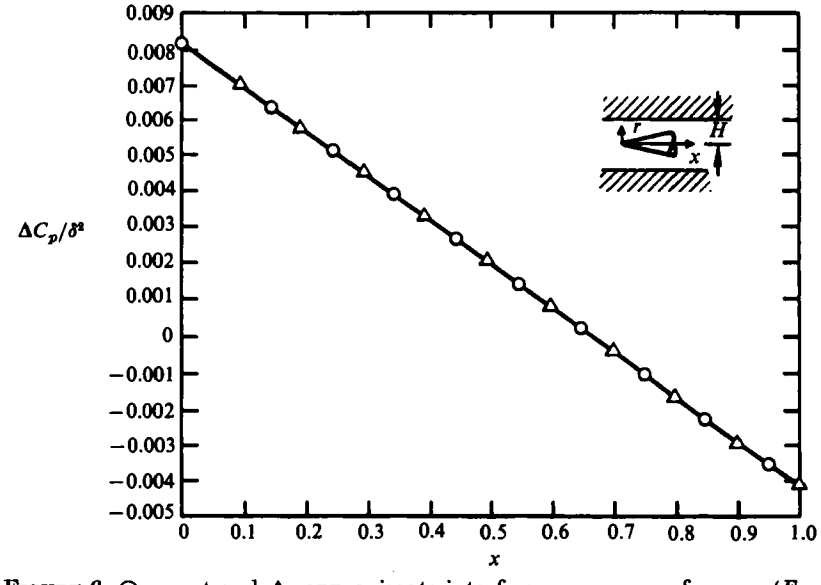

FIGURE 6. ○, exact and △, approximate interference pressures for cone ($F = x$), $H = 4$.

flow described previously. These results show that D'Alembert's paradox applies to closed bodies confined by solid walls. For ventilated walls, this is not correct due to the momentum flux out of the walls.

4. Validations of approximate theory

From the analytical results presented in this paper, it is evident that the asymptotic theory gives a dramatic simplification of the exact theory. To understand its field of application for not-so-large values of H, calculations were performed with

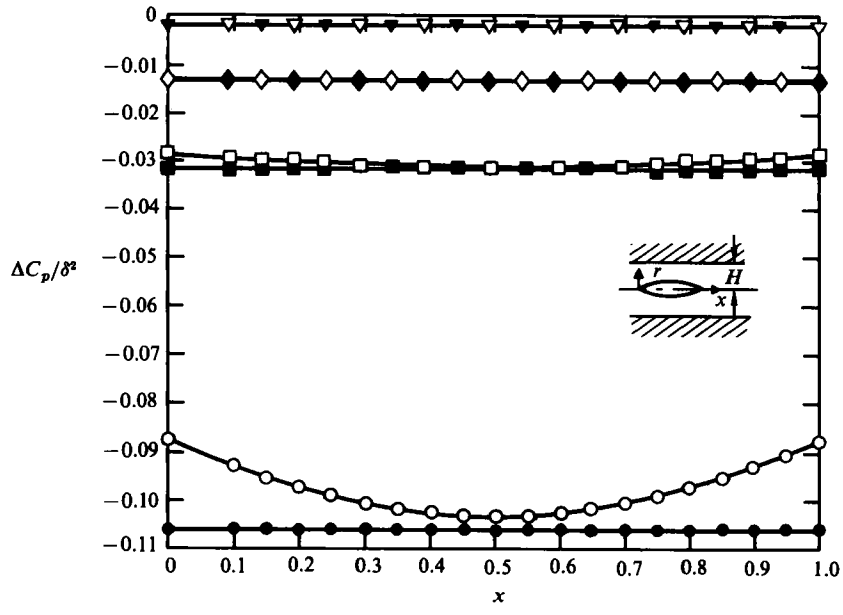

FIGURE 7. Exact and approximate interference pressures for parabola of revolution ($F = 2x(1-x)$). ○, exact, $H = 1$; ●, approx. $H = 1$; □, exact, $H = 1.5$; ■, approx. $H = 1.5$; ◇, exact, $H = 2$; ◆, approx. $H = 2$; ▽, exact, $H = 4$; ▼, approx. $H = 4$.

simple equivalent bodies of revolution that could be considered as representative of more complex shapes. The trapezoidal rule was used to evaluate the rather formidable-looking integrands associated with the exact interference theory given by (21). These integrations were more tractable than expected, since the rapid (exponential) decay of the Bessel function quotient quenched out any oscillations from the sine factor before they could be a problem for large t. Numerical results demonstrating the applicability of the scheme in H space are shown in figures 5–7. In figure 5 the exact and approximate expressions from (21) and (52) are compared for a confined cone. In spite of the extremely low value of H for the $H \to \infty$ theory, the approximate representation tracks the exact value surprisingly well. For $H = 4$, the agreement between both representations is perfect, as shown in figure 6. A similar comparison for a parabolic arc of revolution is shown in figure 7, indicating the same kind of excellent agreement. This behaviour is probably related to the rapid three-dimensional decay of the flow disturbances from slender bodies. It is anticipated that the asymptotic theory for analogous transonic flows may have similar elasticity in its H validity, providing that the supersonic bubble is not too close to the wall region.

5. Conclusions

As asymptotic theory of subsonic flow over slender bodies confined within cylindrical solid wind-tunnel walls has been developed. The theory indicates that the interference pressure on the body is constant for closed bodies. For open bodies, it is a linear function of the streamwise coordinate. This variation upstream and downstream of the body should be modified to account for the non-uniformity at upstream and downstream infinity. For the interference drag, D'Alembert's paradox

holds for closed bodies confined by solid walls. For open shapes, the modification of the static drag is proportional to the product of the base area and blockage ratio. Numerical studies oriented toward assessing the practical application of the asymptotic theory show that it can be used for height-to-chord ratios close to unity with surprising accuracy to predict interference pressures on slender bodies.

REFERENCES

BATCHELOR, G. K. 1967 *Introduction to Fluid Dynamics*, pp. 124–130. Cambridge University Press.

BERNDT, S. B. 1977 Inviscid theory of wall interference in slotted test sections, *AIAA J.* **15**, 1278–1287.

BLYNSKAYA, A. A. & LIFSHITS, Y. B. 1981 Transonic flows around an airfoil in wind tunnels. *Fluid Dyn.* **15**, 711–718.

CHAN, Y. Y. 1980 Singular perturbation analysis of two-dimensional wind tunnel interferences. *Z. angew. Math. Phys.* **31**, 605–619.

COLE, J. D. 1968 *Perturbation Methods in Applied Mathematics*, pp. 182–193. Blaisdell, Waltham, MA.

COLE, J. D. 1972 Studies in transonic flow, transonic area rule-bodies. *UCLA Rep.* ENG-7257.

COLE, J. D., MALMUTH, N. D. & ZEIGLER, F. 1982 An asymptotic theory of solid tunnel wall interference on transonic airfoils. *AIAA paper* 82-093, presented at the AIAA/ASME Joint Thermophysics, Fluids, Plasma and Heat Transfer Conference, St Louis, MO, June 7–11.

COOK, L. P. & COLE, J. D. 1978 Lifting line theory for transonic flow. *SIAM J. Appl. Maths* **35** (2), 209–228.

FERRI, A. & BARONTI, P. 1973 A method for transonic wind tunnel corrections. *AIAA J.* **11**, 63–71.

GARNER, H. C., ROGERS, E. W. E., ACUM, W. E. A. & MASKELL, E. E. 1966 Tunnel wall corrections. *AGARDograph* **109**.

KRAFT, E. M. & DAHM, W. J. A. 1982 Direct assessment of wall interference in a two-dimensional subsonic wind tunnel. Presented at the *AIAA 20th Aerospace Science Meeting, Orlando, Fla, Jan. 11–13.*

LIFSHITS, Y. B. & FONAREV, A. S. 1978 Effect of flow boundaries on parameters of transonic flows around bodies of revolution. *Fluid Dyn.* **13**, 393–399.

LO, C. F. 1978 Tunnel interference assessment by boundary measurements. *AIAA J.* **16**, 411–413.

LOCK, C. N. H. & BEAVAN, J. A. 1944 Tunnel interference at compressibility speeds using flexible walls of the rectangular high speed tunnel. *British ARC R&M* 2005.

MALMUTH, N. D. & COLE, J. D. 1984 Study of asymptotic theory of transonic wind tunnel interference. *Final Report for Period May 30, 1982 through August 30, 1983, Contract No.* F40600-82-C-0005, *Arnold Engineering Development Center/DOS Report* AEDC-TR-84-8. Tullahoma, TN.

MOKRY, M., CHAN, Y. Y. & JONES, D. V. 1983 Two-dimensional wind tunnel wall interference. *AGARDograph* **281**.

MOKRY, M., PEAKE, D. J. & BOWKER, A. J. 1974 Wall interference on two-dimensional supercritical airfoils using wall pressure measurements to determine the porosity factors for tunnel and ceiling. *NRC (Canada)* LR-575.

PARKER, R. L. & ERICKSON, J. C. 1982 Development of a three-dimensional adaptive-wall test section with perforated walls. Presented at the *AGARD Meeting on Wall Interference in Wind Tunnels, London, UK, May 19–20.*

PINDZOLA, M. & LO, C. F. 1979 Boundary interference at subsonic speeds in tunnels with ventilated walls. AEDC-TR-69-47 (AD 687440), May.

SEARS, W. R. 1974 Self correcting wind tunnels (the Sixteenth Lanchester Memorial Lecture). *Aero. J.* **78**, 80–89.

SICKLES, W. L. & KRAFT, E. M. 1982 Direct assessment of wall interference in a three-dimensional subsonic wind tunnel. AEDC-TRM-82-P27.